07

# InGaP/GaAs/Ge triple-junction solar cell with a thinned germanium substrate

© M.A. Putyato,[1] V.V. Preobrazhensky,[1] B.R. Semyagin,[1] N.V. Protasevich,[1] I.B. Chistokhin,[1] M.O. Petrushkov,[1] E.A. Emelyanov,[1] A.V. Vasev,[1] A.F. Skachkov,[2] V.V. Oleinik,[2] S.V. Yanchur,[3] A.V. Drondin[3]

[1] Rzhanov Institute of Semiconductor Physics, Siberian Branch, Russian Academy of Sciences,
630090 Novosibirsk, Russia
[2] Joint Stock Company „Saturn“,
350072 Krasnodar, Russia
[3] State Scientific Center of the Russian Federation „Keldysh Research Center“,
125438 Moscow, Russia
e-mail: puma@isp.nsc.ru

*Received January 26, 2024*
*Revised March 13, 2024*
*Accepted March 25, 2024*

The creating problems of lightweight flexible InGaP/GaAs/Ge solar cells with a thinned germanium substrate and approaches for their solution are discussed. Design of a lightweight flexible solar cell with a Ge substrate thinned to $40 \times 80$ mm has been implemented, based on 40 mm by 80 mm standard photovoltaic cell with anti-radiation glass $120\,\mu$m thick. Specific weight and ultimate bending radius of the experimental sample was $\sim 0.6\,\mathrm{kg/m^2}$ and — $\sim 54$ mm respectively. It efficiency for AM0 spectrum at the temperature of 28°C is 27.6% with a fill factor of $\sim 83.8\%$. It has been shown that germanium surface passivity by means several silicon atom layers deposited from an atomic flux at temperatures below 80°C reduces the back surface recombination.

**Keywords:** space solar cells, mass-dimensional characteristics, thin solar cells, thin solar cell creation problems.

DOI: 10.61011/TP.2024.05.58523.21-24

## Introduction

Increasing of complexity level of current and future scientific and applied objectives solved in space, and expansion of their list suppose increase in power-do-weight ratio of space vehicles (SV). Main primary source of energy for SV is solar cells (SC). In [1] review of SV SC development is given, and classification is provided of modern designs, tendencies of their evolution are determined. Paper of another team of authors [2] contains the results of calculations of basic absolute and relative operation characteristics of modern and future SC for SV. Systematized information on modern designs of SC, their photogenerating parts (PGP) and developments in sphere of space assembly of structures and additive technologies is given in [3]. According to [1–3] one of the main ways of SV power-do-weight ratio increasing is qualitative improvement of weight-energy and weight-size characteristics of SC, and their volume decreasing in transportation position. This is achieved by efficiency increasing of photovoltaic converters (PVC), decreasing of unit weight of PGP, and ensuring more dense stacking of SC.

The promising materials solution to improve PVC efficiency is use of multi-cascade heteroepitaxial structures (HES) based on compounds $A^{III}B^{V}$, which ensure creation of the converters with better unit weight, size and volume characteristics of power [1–4].

Unit weight of SC can be decreased by use of light and flexible PGP, which structural unit is PVC manufactured based on HES of compopunds $A^{III}B^{V}$, with thinned or completely removed substrate (see [5–7]). During manufacture of light flexible PVC (LFPVC) HES partially or completely free of substrate is transferred to lighter composite carrier. Increased flexibility of such PVC ensures use of the design solutions ensuring large compactness of SC in transported position.

The limit decrease in unit weight of LFPVC under other equal conditions can be achieved in case of substrate complete removal. It is advisable to use thinning of the substrate in case when its absence critically decrease the efficiency and/or reliability of the converter. Note that limit flexibility of LFPVC is mainly determined by the thickness of brittle cover glass, which varies from $50-150\,\mu$m [6].

Theme of creating LFPVC with completely removed substrate is associated with major part of studies. Currently several material materials science and technology directions are under development. In view of possibility to increase the efficiency PVC based on inverted metamorphic HES with InGaAs long-wave cascade or HES with diluted nitrides GaInNAs or GaInAsNSb and direct architecture of layers occupies the leading positions [1–4,7]. Technology of manufacturing LFPVG based on inverted metamorphic HES with InGaAs cascade achieved rather high level. Some manufacturers promote their products [8–10], and since 2017 NASA on the International Space Station tested flexible roll SC ROSA (Roll Out Solar Array), manufactured based on similar LFPVC [1]. Note that studies to improve design and technology of manufacturing LFPVC based on inverted metamorphic structures continue (see [11]).

Implementation at industrial level of the technology of manufacturing PVC based on HES with layers of diluted nitrides is possible in the long term only. This is due to insufficient level of technology development of molecular-beam epitaxy of cascades with diluted nitrides, and the necessity to solve problems of combination of methods of molecular-beam epitaxy (MBE) and MOS hydride epitaxy in same technological complex.

Ides of LFPVC with thinned substrate is implemented worldwide based on heterosystem InGaP/GaAs/Ge, in which the third cascade is formed due to autodoping of the germanium substrate during growth on it of layers of compounds $A^{III}B^{V}$. Theme of InGaP/GaAs/Ge PVC with unthinned substrate is discussed not only in scientific articles, but in dissertation [12,13]. Industrial production of such PVC is well mastered worldwide [4], however, studies on the development of this theme continues currently [12,14]. The listed circumstances, as well as this studies of scientific and applied nature [15–18] determine the attractability of heterostructures InGaP/GaAs/Ge as basis of LFPVC with thinned substrate.

Currently for common space objectives solution AZUR and CESI SpA suggest InGaP/GaAs/Ge PVC with thickness of the semiconductor part $80 \pm 20\,\mu$m. Technical characteristics of such PVC are free accessible at official web-sites [19,20]. In [6] it is stated that for important space missions AZUR can deliver lightweight versions of converters with thickness of semiconductive part $20-50\,\mu$m. Note that developed technology is limited by the layers InGaP/GaAs and Ge total thickness of $20\,\mu$m. Generally HES thickness reaches $\sim 5\,\mu$m, so, minimum thickness of Ge is $\sim 15\,\mu$m. But this thickness is far from values, below which significant deterioration of characteristics of germanium cascade starts. So, papers [17,18] state that Ge thickness can be decreased to $7\,\mu$m without critical decreasing of PVC efficiency. The present paper relates to solution of problems relating creation of InGaP/GaAs/Ge LFPVC with germanium substrate thinned to thickness below $\sim 15\,\mu$m.

## 1. Problems of designing and manufacturing technology of InGaP/GaAs/Ge LFPVC

Let's discuss the problems relating creation of InGaP/GaAs/Ge LFPVC with germanium substrate thinned to thickness $\sim 15\,\mu$m and below. One of such problems is increase in recombination losses on the back side of the germanium cascade as the thickness of the germanium substrate decreases [17]. This complicates achievement of the maximum level of improvement of weight-energy characteristics of LFPVC by its unit weight decreasing. Measures shall be taken to decrease concentration of the recombination cites of minor carriers and to create barrier for them on the back side of the germanium substrate. Concentration of the recombination centers can be decreased by germanium oxides removal from the substrate surface directly before an ohmic contact formation in a metal deposition unit, for example, by ion bombardment. Additional passivation of the germanium surface cleaned of oxides is possible using layers of amorphous and epitaxial silicon [21–24]. But difficulty is that suggested in literature methods with silicon layers deposition suppose the germanium substrate heating to temperature above 300°C. For composite object, which is LFPVC (see below), such heating is inaccessible. The known methods of back barrier formation have the same temperature limitations on applicability. For example, in paper [25] the ohmic contact and the back barrier of separate germanium converter are formed simultaneously by sputtering Al layer and further product annealing to 426°C. Note that ohmic contact formation to germanium of *p*-type is not a complex objective, and its formation does not require significant heating of the product (see [26]).

As per structure InGaP/GaAs/Ge LFPVC is a thin film multi-layer composite structure, which layers are attached with each other by adhesion forces of various nature. The materials used for LFPVC creation differ significantly from each other in their physical, chemical and technological properties, which significantly complicates design and manufacturing technology of the converter. In [27] discussing design and manufacturing technology of two-cascade LFPVC based on InGaP/GaAs/Ge HES with completel;y removed germanium substrate, the authors consider in detail the issues of thermomechanical stresses, technological stability of the converter, as well as the role of polymeric materials in stress compensation. Note that in case of germanium substrate complete removal LFPVC achieves high flexibility [27], limited exclusively by flexibility of the cover glass. This is due large deformation potential $A^{III}B^{V}$ of HES with thickness of $\sim 5\,\mu$m. But experience [27] can not be completely applied to LFPVC with thinned germanium substrate. The problem is brittleness of the germanium layer, which is observed even after thinning to $15\,\mu$m and below.

The carrying element of LFPVC structure, which to a large extent determines its strength characteristics, is film polymeric carrier. Polyimide films are most often used as a base for flexible carrier. This material has required radiation resistance, high mechanical and temperature characteristics. It is used to manufacture aerospace equipment parts and flexible electronics, both independently and as part of composites. More details of advantages and drawbacks of polymide film use as base for the flexible carriers are given in [27]. Here the methods of compensation the polymide film drawbacks both at design, and technological level are suggested.

When developing design and manufacturing technology of LFPVC we need to solve problems relating strengthening and protection of periphery of thinned heterostructure and places of electric leads attachment to it. The critical operation during InGaP/GaAs/Ge LFPVC manufacturing is attachment of electric leads to layers of back metallization of the heterostructure attached on the cover glass via the layer of elastomer. The extreme brittleness of the semiconductor web, and especially its edge console, applies additional

limitations for the allowable level of local thermal and mechanical loads during leads attachment to the metallization layer. Note that design of flexible carrier and electric lead of back contact of LFPVC will be mainly determined by exact features of architecture of flexible PGP and SC as a whole. For example, in paper [15] the option of organization the back contact lead via holes uniformly distributed in the foil-coated web of the polymer carrier over full surface of PVC. Switching of the back contact with foul-coated outer surface of the flexible carrier is provided by soldering using indium through these holes. At that the foil-coated surface can be used to form the elements of the conductor infrastructure. The authors successfully implement the described method of lead connection to the back contact on a fragment of PVC mass-produced at AZUR after the germanium substrate thinning to $\sim 50\,\mu$m. Possibility of such approach use at the substrate thickness below $20\,\mu$m is not obvious and requires verification.

To reduce the probability of destruction of the thinned PVC during technological manipulations it shall be secured on a temporary carrier [16,18]. The cover glass can serve as the temporary carrier. Such approach is suggested in paper [6]. The authors note that strengthening by the cover g;ass is necessary for PVC with semiconductor part thinned to $50\,\mu$m and below. In [16] it is suggested to use the technological carrier even in case when the thinned PVC is already provided with cover glass.

The main problem of the method of thinning the large-area substrate by its dissolving is the selection of the etchant composition and etching modes. The etchant shall have high planar homogeneity of vertical etching rate not depending on nature and degree of surface relief development at macro- and micro-levels. It is desirable that the original surface relief be preserved during the etching process without visible change of its planar and vertical characteristics until the substrate material is completely removed. In this case there is possibility to form light diffusing elements on the substrate surface prior to its thinning and their keeping during thinning. Dependence of dilution rate on time is not critical characteristic. It is important that the etchant has low selectivity with respect to structural defects penetrating the HES (dislocations, stacking faults, microcracks, etc.).

To remove and thin the germanium substrate generally etchants based on hydrofluoric [28–30] or orthophosphoric acids [16,27,31] are used. Use of the etchants based on the hydrofluoric acid is not desirable, as it exhibits high activity towards many structural materials, ans also to tissues of the human body. So, reliable protection of the cover glass, end surface of HES and germanium $p-n$-transition is necessary against destructive effect of the etchant. Etchants based on orthophosphoric acid are more preferable. Regardless the etchant composition for the substrate thinning it is expedient to use method of chemical-dynamic etching (see [30]). Previously for Ge substrate complete removal we used two-stage technology of chemical-dynamic etching [27]. Modes selected in [27] generally correspond to the above specified requirements.

Note that experimental studies aimed to solve the problems of design and manufacturing technology development for LFPVC are generally implemented using model samples with simplified design with relatively small dimensions. Approaches successfully implemented using simplified scheme cannot always be successfully reproduced when applied to full-size PVC. So, it is expedient to perform searches based on standard full-size PVC. It is also important that the suggested solution will have the potential of their adaptation to conditions of PVC mass production.

## 2. Design of experimental InGaP/GaAs/Ge LGPVC

Design and manufacturing technology of the experimental LFPVC were developed based on InGaP/GaAs/Ge solar energy converter with form factor $40 \times 80$ mm and germanuium substrate $145\,\mu$m thick mass produced at JSC „Saturn“İnitial PVC used for LFPVC manufacturing were equipped with radiation protection glass $120\,\mu$m thick, electrical leads of face contact and shunt diode, but did not have back layers of ohmic contact and metallization. The initial PVC were manufactured completely as per the standard technology using standard components and materials.

The layout diagram of the experimental LFPVC is presented in Fig. 1. Thick contour line shows the standard PVC with thinned germanium substrate. LFPVC architecture is made around the semiconductor heterostructure. Herein the heterstructure means a complex comprising germanium substrate *1* and HES $A^{III}B^{V}$ *2*. On HES upper side a system of face contacts is formed *5*, and anti-reflective coating (not shown in Figure). Flexible electric leads are connected to mesh of face contacts *6*. PVC face side is covered by cover glass of radiation protection *4*. The cover glass is attached using transparent glue *3*. On back side the thinned germanium substrate a solid ohmic contact is formed, and layers of back metallization *11* are applied, the flexible electric lead *16* is connected to them. The end periphery of HES and Ge $p-n$-transition are protected with dielectric layer *10*. The supporting base of LFPVC is the composite flexible carrier *14*, formed on the basis of polymer film. The flexible carrier is attached to the back side of PVC via a layer of adhesive *13*. The design takes into account the need to increase the reliability of the face electrical leads attachment. For this the lead bases are attached by adhesive tie *7* to the glass and layer of transparent glue, squeezed out in some quantity from the gap between the glass and the heterostructure when they are mated at stage of initial PVC manufacturing. Before the tie formation, a reagent is applied to the attachment points to increase the materials adhesion. All periphery of thinned PVC is protected against physical-chemical action during manufacturing and testing of LFPVC *9*. Strengthened attachment of PVC to flexible carrier is provided along the periphery of the cover glass to reduce the probability of delamination of LFPVC composite

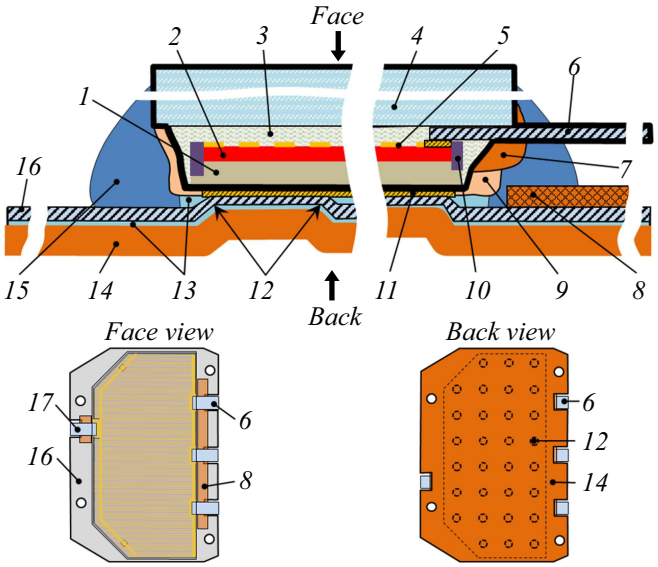


**Figure 1.** Layout diagram of experimental LFPVC: *1* — thinned Ge substrate, *2* — $A^{III}B^{V}$ HES, *3* — transparent glue layer, *4* — glass, *5* — face contact, *6* — flexible lead of face contact, *7* — Additional attachment of face contact lead, *8* — isolating insert, *9* — strengthening of periphery of thinned PVC, *10* — Layer of passivation of HES periphery and $p-n$-transition of germanium cascade, *11* — back contact, *12* — contact pad of back contact lead, *13* — silicon compound, *14* — polyimide film, *15* — additional fixing of periphery of thinned PVC to carrier, *16* — back contact lead, *17* — shunt diode lead.

structure under action of loads occurred during its bending and twisting *15*.

The flexible carrier and the back contact lead are assembled into a single composite thin-film structure. The support base of the structure is polymide film 25 $\mu$m thick *14*, to it the aluminium foil 10 $\mu$m thick is glued. On composite web of the flexible carrier the uniformly distributed array of convexes is formed protruding to height of 20 $\mu$m above its plane at side of the aluminium layer. Peaks of convexes *12* are contact pads for leads. The contact pads distribution over the back surface of PVC is shown in image of LFPVC back side (see „Back view“ in Fig. 1). The mechanical electric contact between the lead and the metallization layer of LFPVC is formed by pressing the array of contact pads to layer of back metallization *11* during the flexible carrier adhesion to PVC in vacuum. The force of elastic contact pads pressing to the back metallization is ensured by deformation of their three-dimensional profile. The flexible carrier is fixed to PVC using glue layer applied on the flat aluminium surface between the convexes.

## 3. Manufacturing of LFPVC samples

Two groups of samples were prepared. One — without thinning of the germanium substrate, and another one — with its thinning. Each group comprises samples both with silicon sublayer, and without it. Group of thinned PVC comprises two samples. The sample with sublayer of silicon is designated as $A^{Si}$, and without sublayer — $A$. LFPVC group comprises 4 samples. Two samples with sublayer of silicon ($B_1^{Si}$ and $B_2^{Si}$) and two samples without sublayer of silicon ($B_1$ and $B_2$). Samples with thinned germanium substrate differ from each other by thickness of germanium cascade ($D$) and by amount of deposited silicon ($Q$). As unit of measurement $Q$ the atomic monolayer (AML) is selected. One AML corresponds to number of atoms required to fill all lattice nodal positions on the plane Ge(001). Data relating residual thicknesses of the germanium substrates and amount of deposited silicon are given in Table 1 (see Sec. 4).

### 3.1. Substrate thinning

Route of LFPVC manufacturing starts from germanium substrate thinning. Thinning is performed by chemical-dynamic etching in a solution based on orthophosphoric acid, hydrogen peroxide and water. PVC is attached to the reusable film technological carrier using adhesive layer based on organosilicon compounds. Technological carrier with PVC is transported onto the object table of the etching unit. During thinning the table executes plane-parallel planetary motion relative to the inclined axis of rotation of the etching bath. The bath contains additional structural elements ensuring intensive motion of liquid above the surface of the germanium substrate. Time for removal of 135 $\mu$m germanium is about 3.5 h. During etching the solution is not updated. Average rate of etching is $\sim 0.62\,\mu$m/min at 23°C. The etchant composition, solution temperature, modes of its stirring and flow above the sample surface ensure uniform removal of germanium over full surface of PVC. Maximum height difference of the residual portion of the substrate during removal of $\sim 140\,\mu$m of material is estimated to be about 5 $\mu$m.

Quality of removed material is monitored using easy removable satellite-sample attached directly near one of sides of PVC. The satellite is manufactured by glueing the heterostructure without cover glass to the silicon mandrel using non-shrink epoxy adhesive. During removal of $\sim 75\%$ of germanium to be dissolved the check measurement of satellite-sample thickness is performed, and time required to complete the process is calculated. Thickness is measured by a micrometer. Final thickness check of residual germanium layer cane be performed by optical microscopy methods using sections of transverse chips of satellite-sample. Fig. 2 shows photo of cross-section of satellite-sample with $D \approx 6.5\,\mu$m.

### 3.2. Germanium surface passivation by silicon atoms

Experiments were performed on passivation of oxidized surface of thinned germanium substrate with ultra-thin layers of silicon formed from atomic flow in ultra-high

**Table 1.** Characteristics of samples of PVC and LFPVC

| Sample | $D$ $\mu$m | $Q$ AML | $I_{SC}$, A | $U_{OC}$, V | $I_{P\max}$, A | $U_{P\max}$, V | $P_{\max}$, W | $FF$, % | $\eta_{\max}$ % |
|---|---|---|---|---|---|---|---|---|---|
| $C$ | 145 | 0 | 0.516 | 2.686 | 0.499 | 2.42 | 1.208 | 87.13 | 29.3 |
| $A$ | 145 | 0 | 0.518 | 2.661 | 0.498 | 2.348 | 1.169 | 84.84 | 28.36 |
| $A^{Si}$ | 145 | 6 | 0.520 | 2.652 | 0.499 | 2.348 | 1.172 | 82.02 | 28.43 |
| $B_1$ | $\sim 15$ | 0 | 0.523 | 2.622 | 0.490 | 2.263 | 1.109 | 80.80 | 26.89 |
| $B_2$ | $\sim 8$ | 0 | 0.520 | 2.609 | 0.481 | 2.263 | 1.089 | 80.16 | 25.82 |
| $B_1^{Si}$ | $\sim 10$ | 6 | 0.520 | 2.613 | 0.497 | 2.292 | 1.139 | 83.78 | 27.60 |
| $B_2^{Si}$ | $\sim 10$ | 9 | 0.522 | 2.575 | 0.501 | 2.264 | 1.134 | 84.45 | 27.52 |

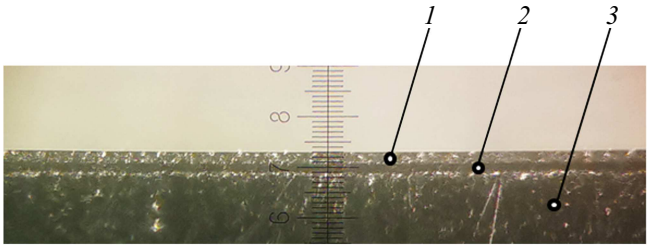


**Figure 2.** Cross-section of satellite-sample with thinned to $\sim 11\,\mu$m InGaP/GaAs/Ge heterostructure without anti-reflecting layers and face contact infrastructure. The ruler division is $5\,\mu$m. *1* — heterostructure, layers $A^{III}B^{V}$ HES and germanium substrate have same contrast, *2* — glue layer, *3* — silicon mandrel.

vacuum conditions at a temperature not exceeding 80°C. Passivation was performed prior to application of the ohmic contact and metallization layers.

Samples before loading into vacuum were treated in the etchant based on orthophosphoric acid, the composition of which differed from the composition of the etchant used to thin the substrate. Treatment was performed to create on the germanium surface of the relief satisfying the requirements of epitaxy from molecular flow into two-dimensional layer mode, and to form thin oxide layer.

The silicon layers were grown in machine for MBE of compounds $A^{III}B^{V}$. To form silicon atoms flow the crucible source was used intended to alloy the layers of compounds $A^{III}B^{V}$. Rate of silicon deposition was 0.017 AML/s (atomic monolayer per second). Special heating of samples was not applied, but due to heat radiation of the silicon source the samples temperature increased to values not exceeding 80°C. Note that samples comprising polymer materials, used for LFPVC manufacturing, can be heated to 160°C not disturbing conditions of ultrahigh vacuum, which was identified as result of the preliminary experiments.

The surface state of germanium in MBE machine was monitored by reflected high-energy electron diffraction (RHEED). In RHEED pattern from initial surface we observed relatively intensive and narrow reflexes from Ge face (001) without structural features. Point reflexes Point reflections from transmission diffraction and signs of surface faceting were absent at all azimuths. During deposition of first 2–3 AML the clarity of linear reflexes increased somewhat. Upon further $Q$ increasing the diffuse background began to increase.

Samples with deposited silicon were handed over for formation of ohmic contact and metallization layers after they were held under normal conditions in atmosphere during one day. Additional chemical treatment and ionic cleaning of samples with silicon sublayer were not performed.

### 3.3. Formation of ohmic contact and metallization contacts

Unalloyed ohmic contact on samples both with and without the silicon sublayer was formed based on titanium by vacuum sputtering. Samples temperature did not exceed 80°C. Unmonitored samples heating was determined by heat radiation of the metal sources. Total thickness of layers of back metallization did not exceed $0.5\,\mu$m. Samples whithout silicon sublayer before loading into vacuum were treated in the etchant based on orthophosphoric acid and additionally cleaned by ionic bombarding just before the ohmic contact formation. The etchant composition and processing modes are identical to the samples preparation for silicon deposition.

### 3.4. LFPVC assembly

After the metallization layers application the flexible carrier with back contact lead was glued to samples. The flexible carrier connection with PVC was made by vacuum lamination. For this atmosphere was removed from the gap between the flexible carrier and PVC. The uniformly distributed load created by atmospheric pressure through a silicone membrane was then applied to the flexible carrier. In case of unthinned samples the flexible carrier and external lead of back contact were not used, as the strength of thick germanium substrate ensures measurements without risk of the heterostructure damage on back side, and bending tests of these samples were not expected.

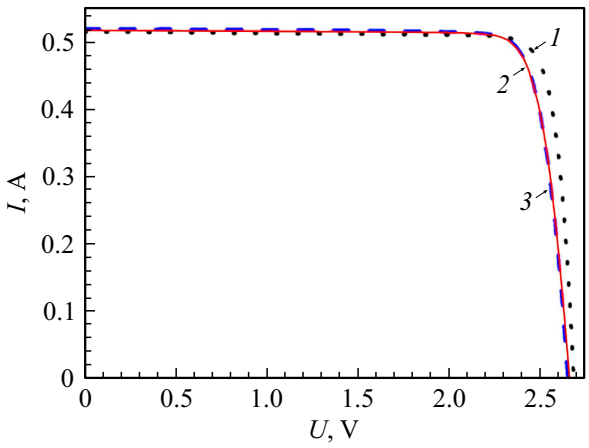


**Figure 3.** CVC of PVC with unthinned substrate: *1* (dots) — sample *C*; *2* (solid line) — PVC without silicon sublayer, *A*; *3* (dashes) — PVC with silicon sublayer, $A_{Si}$.

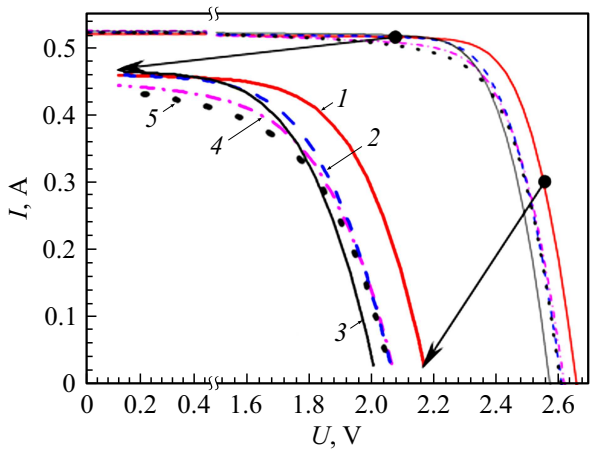


**Figure 4.** CVC: *1* (thick line) — sample *A*, *2* (dashes) — $B_1^{Si}$, *3* (thin line) — $B_2^{Si}$, *4* (dot-dash) — $B_1$, *5* (dots) — $B_2$.

## 4. Properties of experimental LFPVC

### 4.1. Current-voltage curves of samples

Samples of LFPVC and PVC with unthinned substrate were tested at simulator of sun radiation AM0 of permanent burning at object table temperature 28°C. To fix LFPVC on the object table the vacuum clamp was used. Under conditions of continuous illumination some overheating of the semiconductor part of LGFEP was possible in relation to the object table temperature due to the flexible composite carrier presence between it and the object table. But due to low thickness of the flexible carrier (some tens of $\mu$m) and the layer of aluminum foil included in its composition, and having good thermal conductivity, the possible overheating was not considered.

Table 1 presents basic photovoltaic characteristics of the experimental samples and reference (standard) PVC designated in Table with symbol *C*: short circuit current — $I_{SC}$; no-load voltage — $U_{OC}$; current and voltage at point of maximum power — $I_{P\max}$ and $U_{P\max}$ respectively; maximum power — $P_{\max}$; CVC filling factor — $FF$; converter efficiency in point of maximum power — $\eta_{\max}$. Also data on thicknesses of germanium cascades $D$ and amount of deposited silicon $Q$ are provided.

Fig. 3 shows CVC of unthinned samples *A* and $A^{Si}$, and reference PVC *C*. Properties of samples of type *A* are very close to each other (see lines *2* and *3*). Some increase in value of $\eta_{\max}$ at transition from *A* to $A^{Si}$ (Table 1) can not be unambiguously associated with the effect of silicon sublayers.

Observed difference of CVC of samples *A* and $A^{Si}$ from curve of reference sample is due to presence in them of series resistor, which is explained, probably, by low thickness of metallization layers of PVC *A* and $A^{Si}$. Their back metallization was equal to $\sim 0.5\,\mu$m only, opposite to metallization of sample *C* equal to several $\mu$m.

LFPVC CVC are shown in Fig. 4. Thinned samples $B_1^{Si}$, $B_2^{Si}$, $B_1$ and $B_2$ have lower values of no-load voltage as compared to samples of type *A* (Table 1). Characteristics of sample $B_1$ with $D = 15\,\mu$m are somewhat better than characteristics of sample $B_2$ with $D = 8\,\mu$m. Differences are observed in relation to $FF$, $P_{\max}$ and $\eta_{\max}$. But in this case we can not make unambiguous conclusion that differences in values of characteristics are due to differences in thicknesses of the residual germanium layer — for this we have low data relating $D$ effect on LFPVC properties.

Comparison of curves in Fig. 4, and data of Table 1 ensure conclusion that LFPVC samples with silicon sublayer have higher photovoltaic characteristics than samples without sublayer. The low value of the no-load voltage of $B_2^{Si}$ sample in relation to other LFPCVs is noteworthy (Fig. 4, line *3*). Nevertheless values $FF$ and $\eta_{\max}$ of sample $B_2^{Si}$ are comparable with values of the appropriate characteristics of sample $B_1^{Si}$. As per structure the samples $B_2^{Si}$ and $B_1^{Si}$ differ by value $Q$ only. Amount of the deposited silicon in case of sample $B_2^{Si}$ is by 1.5 times higher than in case of $B_1^{Si}$ (Table 1).

### 4.2. Weight and size characteristics of LFPVC

Table 2 shows weight and size characteristics of LFPVC $B_1^{Si}$, and its components.

According to Table 2 thinning of the germanium substrate to $10\,\mu$m ensures decreasing of weight and size characteristics of converter under the paper implemented design and technological solutions by $\sim 2$ times as compared to standard PVC. The weight and size characteristic of LFPVC $B_1^{Si}$ in point of maximum power is $\sim 632.8$ W/kg, and of standard PVC — $\sim 327.40$ W/kg.

### 4.3. LFPVC flexibility test

The experimental LFPVC was bend tested using cylindrical mandrel with diameter of 108 mm (Fig. 5). During

**Table 2.** Weight and size characteristics of the initial PVC, LFPVC $B_1^{Si}$ and its components

| Parameter | Unit of measurement | Parameter value |
|---|---|---|
| Weight of standard PVC with size 40 × 80 mm and germanium substrate with thickness 145 $\mu$m, cover glass ∼ 120 $\mu$m thick, flexible leads and layers of back metallization | g | ∼ 3.69 |
| Weight of initial PVC with size 40 × 80 mm with germanium sibstrate with thickness 145 $\mu$m, cover glass ∼ 120 $\mu$m thick, flexible leads, but without layers of back metallization | g | ∼ 3.45 |
| Area of initial and standard PVC | $cm^2$ | 30.17 |
| Area of cover glass of initial and standard PVC | $cm^2$ | ∼ 30.41 |
| HES thickness | $\mu$m | ∼ 4.50 |
| Residual thickness of LFPVC germanium substrate | $\mu$m | ∼ 10 |
| Thickness of flexible carrier web (not considering height of contact pads) | $\mu$m | ∼ 50 |
| Total thickness of LFPVC (considering height of contact pads) | $\mu$m | ∼ 250 |
| Weight of thinned PVC | g | ∼ 1.28 |
| Weight of flexible carrier of FLPVC | g | ∼ 0.50 |
| Total weight of LFPVC | g | ∼ 1.80 |
| Weight of FLPVC reduced to area of initial PVC | $kg/m^2$ | ∼ 0.60 |
| Weight of standard PVC reduced to its area | $kg/m^2$ | ∼ 1.22 |

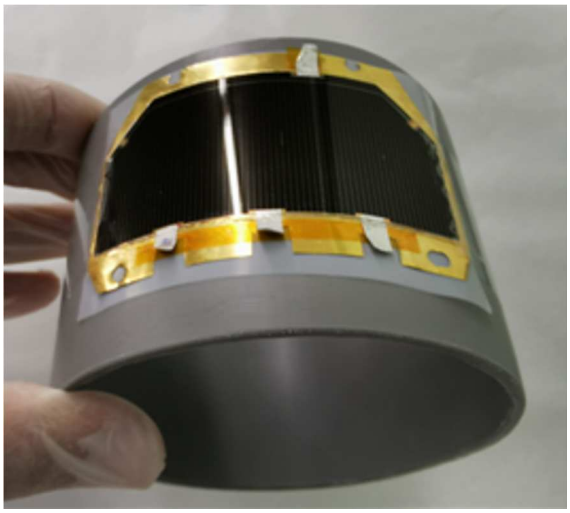

**Figure 5.** LFPVC attached on mandrel with diameter of 108 mm.

testing one of short sides of LFPVC was fixed on the mandrel along the glass edge using strip of adhesive tape. Further the converter was pressed in series to the mandrel by force distributed along the contact line between LFPVC and mandrel, with gradual shift of this force from the secured edge of LFPVC to free edge. Single deformation cycles have no visible effect on LFPVC characteristics. Test for resistance to multiple bending was not performed as design and manufacturing technology of LFPVC at this study stage were not optimized for this objective.

It was found that the bending radius of 54 mm is very close to the critical one for this design of LFPVC and glass thickness 120 $\mu$m. This is confirmed by the glass destruction near its transverse axis of symmetry at insignificant radial deformation of the mandrel, increasing its curvature at LFPVC location. When mandrel of somewhat larger diameter is used such effect was not observed.

## 5. Discussion of results

### 5.1. Design

Architecture of experimental LFPVC was not optimized by composition, thicknesses and method of components interfacing. The suggested solutions are experimental. So, design of the flexible carrier and method of its interfacing with the converter ensured the problem solution of reliable connection of electric leads to the back contact of PVC with germanium substrate thinned to below 15 $\mu$m. The suggested approach is suitable to manufacture the experimental samples of full-size LFPVC and to test them at laboratory level. However, its applicability for the manufacture of LFPVC intended for use in actual conditions is not obvious and requires study. Generally, LFPVC design requires further comprehensive studies directed on its optimization to increase the converter resistance to aby effects, including contact loads from the flexible carrier side.

### 5.2. Germanium substrate thinning

The above evaluation of etching heterogeneity given as heights difference 5 $\mu$m upon deletion of 140 $\mu$m Ge, probably, is overestimated. Direct measurement of sample thickness over its area using the mechanical instruments was difficult due to extreme brittleness and low rigidity of ultra-thin heterostructure laying on elastic glue layer about 25 $\mu$m thick. So, evaluation was made by etching rate and time period between moment of first window

appearance in germanium, which provides access to layers $A^{III}B^{V}$, and moment of complete removal of all substrate traces visible by naked eye. Measurements of sample thicknesses over its area at reference thickness of substrate $\sim 50\,\mu$m provide evaluation of heights difference $3\,\mu$m at linear extrapolation of the obtained data to $140\,\mu$m of removed material. Note that it is advisable to thin PVC on which the front contact leads and the shunt diode are already installed. This requires measures protecting leads from etching solution flow, and decreasing local disturbing effect of their protection elements on the fluid flow modes. To increase homogeneity of etching it is necessary to improve design of the chemical-dynamic etching unit. and to optimize the etchant flow modes.

One of features of technology use of germanium substrate thinning is reproduction of the original surface macrorelief without visible changes in its geometry up to the complete removal of the material. Keeping of the relief pattern is observed at the background of increasing of surface reflectivity, i.e. surface smoothening is performed at level of relief elements with dimensions below $1\,\mu$m. Probably, etching is implemented using layer-by-layer dissolving of terraces with orientation (001) during localization of processes of material dissociation along their edges.

Main factors determining density of the recombination cites are composition and structure of oxide layer, and structure of interface between it and semiconductor. The interface properties are significantly affected by the surface relief of the crystal at level of atomic terraces and their systems. The terraces are formed both due to the substrate deviation from singular face (001), and due to violations of surface flatness. Irregularity of edges of the terraces and the presence of small pits and protrusions of nanometer size on their surface are undesirable elements of the relief even in the absence of oxide. Due to this after the substrate thinning additional finish etching of the germanium surface was performed to improve the surface relief ordering at level of terraces system.

As it was mentioned above, on RHEED pattern from the initial surface only basic linear refluxes of the face (001) are observed, at that point reflexes and signs of faceting were absent. This means that surface of the thinned substrate is formed by terraces system (001) without tree-dimensional objects of nanometer-scale, on which the transmission diffraction and facets formation can be implemented. The observed RHEED pattern ensures the conclusion that on surface there is oxide layer of low thickness, this is confirmed by relatively high intensity and small width of the basic linear reflexes upon absence of overstructural features. So, selected mode of chemical-dynamic etching and additional etching of surface just before samples location in vacuum ensured significant decrease in relief development at the level discussed above, and formation of thin oxide layer.

### 5.3. Passivation of germanium surface and photovoltaic properties of LFPVC

Selection of the passivation method of oxidized germanium surface using silicon atoms deposited under conditions of ultra high vacuum from atomic flow, is determined by data of papers [21,32,33]. As, in [21] possibility of epitaxial layers of silicon to decrease concentration of surface states of germanium, and optimal conditions of such layers formation are discussed. The authors [33] demonstrated high reducing activity of silicon atoms arriving at the oxidized surface of GaAs under ultra high vacuum conditions in the form of atomic flow. It turned out that the silicon atoms can restore GaAs oxides even at room temperature. Paper [32] showed that the epitaxial films of silicon with thickness of several atomic monolayers, grown by MBE method on surfaces GaAs (001) and (111) prevent the crystal oxidation in atmosphere. We suppose that as a result of interaction of silicon atoms flow and oxidized surface of germanium its oxide modification will occur with decrease in concentration of free states, and protective film will be formed preventing further oxidation of the substrate in atmosphere.

Data obtained in this paper ensure conclusion that silicon atoms entering germanium surface in number equivalent to several atomic monolayers modify the oxide layer and prevent its thickness increasing upon further holding in atmosphere. We believe that modification of the oxide layer facilitates decreasing of minor carriers recombination on the back side of thinned germanium substrates. Fig. 6 shows the normalized CVC of LFPVC and PVC with substrate $145\,\mu$m thick for AM0 (Table 1). CVC of LFPVC with $D \geq 10\,\mu$m form two groups of lines: {2, 3} and {4, 5}.

LFPVCs with silicon sublayer have higher characteristics (lines *2*, *3* in Fig. 6, Table 1). In present paper the detailed analysis of CVC was not performed due insufficient statistics of samples in each group. Join analysis of CVC of large number of LFPVC with identical design is necessary

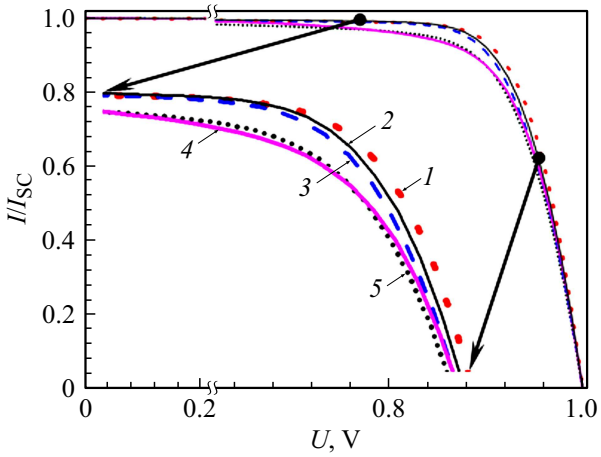


**Figure 6.** Normalized CVC: *1* (bold dots) — sample $A^{Si}$, *2* (thin solid line) — $B_2^{Si}$, *3* (dashes) — $B_1^{Si}$, *4* (thick solid line) — $B_2$, *5* (small dots) — $B_1$.

considering nuances of their manufacturing technology and state of periphery of thinned heterostructure.

Let's discuss the possible mechanism of silicon atoms effect on the oxide layer of germanium surface, based on RHEED data. Considering high restoration ability of the silicon atoms we can suppose that silicon atoms approaching the surface enter in oxidation-reduction reactions, which change composition and structure of oxygen containing layers, including on heterboundary germanium−oxide. Efficiency and mechanisms of exchange heterogeneous reactions are monitored by molecular form, in which silicon enters the surface. Individual adsorbed atoms enter in exchange reactions more effectively, and mechanism of reactions is easier. During formation of solid polycrystalline or amorphous film of silicon the exchange processes will occur even between solid phases. Their rate can be lower than rate of reactions between individual adsorbed atoms and near-surface layers of oxide, so the density of silicon atoms flow shall be agreed with rate of exchange reactions. In our case MBE method ensures monitoring with high accuracy of mass transfer processes on surface. Change of structure of oxide layer upon interaction with silicon atoms can be evaluated by short-term width decreasing of the linear reflexes of RHEED pattern during deposition of first 2−3 AML. The further process of the surface holding in the silicon flow was accompanied by a gradual increase in the diffuse background of the RHEED pattern. Presumably, the active phase of properties changing of the oxide was completed by this time moment, and silicon atoms began to accumulate on the surface in the form of the amorphous or polycrystalline layer. It is difficult to determine the structure of the upper part of the silicon layer using RHEED method due to its small thickness.

Paper shows that amount of silicon deposited on the germanium surface has meaning. This is confirmed by no-load voltage decreasing in case of sample with $Q \approx 9$ AML as compared to samples with $Q \approx 6$ AML, and samples without silicon sublayer (Table 1, Fig. 4). The effect, probably, is due to that with thickness increasing of the silicon layer it tunnel transparency decreases, and the hole barrier begins to contribute. Note that in MBE machine $A^{III}B^{V}$ there is always a background of fifth group elements, so the silicon layer can capture some number of atoms of arsenic or phosphorus. In case of single-crystal or polycrystalline structure the silicon film can comprise donor levels, which in Ge/Si system can result in barrier formation for holes during transition from germanium to silicon. The barrier height will depend on doping level, mechanical stresses, thickness of silicon film and its structure [34]. In order to compensate for the donor impurity, the silicon film can be doped with atoms of the third group.

In paper [25] the authors for simultaneous formation of the back ohmic contact and back barrier of individual germanium converter we used aluminium layers with further sample annealing to 426°C. high temperature of annealing it is prohibited to use directly the suggested approach during LFPVC manufacturing. remind that high technological limit of LFPVC heating under ultra high vacuum dose not exceed 160°C. But aluminium atoms, like silicon atoms, have high reducing properties. In this relation it is interesting to study of possibility of combined use of flows of silicon atoms and aluminium atoms for surface passivation, formation of back barrier and ohmic contact.

## Conclusion

The design of experimental LFPVC is developed based on PVC InGaP/GaAs/Ge with form factor $40 \times 80$ mm and thickness of germanium substrate 145 $\mu$m mass produced at JSC „Saturn". Samples of LFPVC are manufactured with thinned to $\sim 15$, $\sim 10$ and $\sim 8$ $\mu$m germanium substrates and thickness of cover glass $\sim 120$ $\mu$m.

The manufacturing technology is based on results of literature data analysis and available in ISP SB RAN experience of LFPVC manufacturing based on InGaP/GaAs/Ge structures with complete removal of germanium substrate [27]. Design and manufacturing technology of the experimental LFPVC are developed and implemented to initial PVC with cover glass, electric leads of face contact and shunt diode, but without back ohmic contact and metallization layers.

Technology of chemical-dynamic thinning of PVC germanium substrate is tested. Problems of ensuring homogeneity of etching, quality of obtained surface, keeping integrity and operation characteristics of pre-installed structural elements of PVC are solved. Height difference over surface during the germanium layer removal $\sim 140$ $\mu$m thick does not exceed 5 $\mu$m. The etchant is prepared based on orthophosphoric acid and hydrogen peroxide. Average etching rate over time during selected modes of fluid flow above the substrate surface is 0.62 $\mu$m/min at 23°C. Surface structure of thinned germanium substrate at microlevel corresponds to the requirements necessary to implement the epitaxial processes using molecular flows.

Experiments are performed on passivation of germanium surface with thin oxide layer by deposition using method of MBE of silicon atoms in number equivalent to several atomic monolayers. It is shown that silicon atoms deposited on the surface at temperature below 80°C, interact with the oxide layer and change its properties. The oxide layer modification, probably, ensures decreasing of the recombination losses on the back surface of thinned germanium substrate. There is possibility to optimize conditions of germanium surface passivation on flow of silicon atoms under ultra high vacuum in temperature range of 80 to 160°C.

Tests for bending strength of LFPVC with germanium layer $\sim 10$ $\mu$m show that at thickness of cover glass 120 $\mu$m the critical band radius of the experimental converter with overall dimensions $40 \times 80$ mm is close to 54 mm. To reduce the bend radius it is necessary to decrease thickness of cover glass, for example, to 90−50 $\mu$m.

Suggested and tested approaches to problem solution of manufacturing technology of InGaP/GaAs/Ge LFPVC

are promising and require further development as per the following directions:

1. Study of possibility of germanium surface passivation and formation on it of back barrier and ohmic contact with combined use of atomic flows of silicon and aluminium.

2. Improvement of LFPVC in terms of its architecture, materials used and manufacturing technology to increase its strength under bending, twisting and contact deformations from the flexible carrier side.

3. Optimization of modes of chemical-dynamic thinning of substrate to increase homogeneity of etching rate over its surface.

### Conflict of interest

The authors declare that they have no conflict of interest.

## References


[1] Z.A. Kazantsev, A.M. Eroshenko, L.A. Babkina, A.V. Lopatin. Spacecrafts Technol., **5** (3), 121 (2021). DOI: 10.26732/j.st.2021.3.01

[2] M.V. Ryabtseva, A.A. Lebedev, A.A. Naumova, A.M. Bolotin, N.T. Vagapova, P.G. Cherenkov. Inzhenerny zhurnal: nauka i innovatsii, **3**, 1 (2022). (1) (in Russian). DOI: 10.18698/2308-6033-2022-3-2162

[3] A.V. Drondin, A.M. Protasov, A.V. Semenkin, A.A. Shevdin, S.V. Yanchur. Kosmonavtika i raketostroenie, **6** (123), 105 (2021). (in Russian)

[4] E.V. Slyshchenko, A.A. Naumova, A.A. Lebedev, M.A. Genali, N.T. Vagapova, B.V. Zhalnin. Sibirsky zhurnal nauki i tekhniki, **19** (2), 308 (2018). (in Russian). DOI: 10.31772/2587-6066-2018-19-2-308-324

[5] D. Shahrjerdi, S.W. Bedell, C. Bayram, C.C. Lubguban, K. Fogel, P. Lauro, J.A. Ott, M. Hopstaken, M. Gayness, D. Sadana. Adv. Energy Mater., **3** (5), 566 (2012). DOI: 10.1002/aenm.201200827

[6] G.F.X. Strobl, L. Ebel, D. Fuhrmann, W. Guter, R. Kern, V. Khorenko, W. Kostler, M. Meusel. *Proc. IEEE 40th Photovoltaic Specialist Conference* (Denver, CO, USA, 2014), 3595-36002014, DOI: 10.1109/PVSC.2014.6924884

[7] N.A. Pakhanov, V.M. Andreev, M.Z. Schwartz, O.P. Pchelyakov. Avtometriya, **54** (2), 93 (2018). (in Russian) DOI: 10.15372/AUT20180211

[8] *THE AIR FORCE RESEARCH LABORATORY.* Electronic source. Available at: https://afresearchlab.com/technology/space-vehicle/roll-out-solar-arrays (Date of access: 05.07.2023)

[9] *MicroLink Devices.* Electronic source. Available at: http://mldevices.com/index.php/news?start=4 October 24, 2017 (date of access: 05.07.2023)

[10] *Sharp Energy Solutions Corporation (SESJ).* Electronic source. Available at: https://global.sharp/solar/en/high-efficiency/ (date of access: 05.07.2023)

[11] J. Schön, M.M. Gunther, W. Bissels, P. Mulder, R.H. van Leest, N. Gruginskie, E. Vlieg, D. Chojniak, D. Lackner. Progr. Photovoltaics: Res. Appl., **30** (8), 1003 (2022). DOI: 10.1002/pip.3542

[12] A.F. Skachkov, avtoref. kand. t.n. diss. („yuzhno-Rossijskij gos. politekh. un-t (NPI) im. M.I. Platova", Novocherkassk, 2021) (in Russian)

[13] S.A. Mintairov, avtoref. kand. f-m.n. diss. (FTI RAN im. A.F. Ioffe, SPb., 2015) (in Russian)

[14] A.V. Malevskaya, N.D. Ilyinskaya, Yu.M. Zadiranov, A.A. Blokhin, D.A. Malevskiy, P.V. Pokrovskij. ZhTF, **92** (1), 108 (2022). (in Russian). DOI: 10.21883/JTF.2022.01.51860.220-21. [A.V. Malevskaya, N.D. Il'inskaya, Yu.M. Zadiranov, A.A. Blokhin, D.A. Malevskii, P.V. Pokrovskii. Tech. Phys., **67** (1), 82 (2022). DOI: 10.21883/TP.2022.01.52537.210-21]

[15] N.F. Pakhanov, M.Z. Shvarts. SSRN: https://ssrn.com/abstract=4409073 or http://dx.doi.org/10.2139/ssrn.4409073

[16] N.A. Pakhanov, O.P. Pchelyakov, V.M. Vladimirov. Avtometrija., **53** (6), 106 (2017). (in Russian) DOI: 10.15372/AUT20170613

[17] I. Lombardero, M. Ochoa, N. Miyashita, Yo. Okada, C. Algora. Prog. Photovolt. Res. Appl., **28** (11), 1097 (2020). DOI: 10.1002/pip.3281

[18] C. Colin, A. Jaouad, M. Darnon, M. De Lafontaine, M. Volatier, A. Boucherif, R. Arés, S. Fafard, V. Aimez. AIP Conf. Proceed., 1881, 040001-1 (2017). DOI: 10.1063/1.5001423

[19] *AZUR SPACE Solar Power.* Electronic source. Available at: https://www.azurspace.com/images/products/ 0004148-00-01_DB_GBK_80.m.pdf (Date of access: 05.07.2023)

[20] *CESI SpA.* Electronic source. Available at: https://www.cesi.it/app/uploads/2020/03/Datasheet-CTJ30-Thin.pdf. (access date: 05.07.2023)

[21] B. De Jaeger, R. Bonzom, F. Leys, O. Richard, J. Van Steenbergen, G. Winderickx, E. Van Moorhem, G. Raskin, F. Letertre, T. Billon, M. Meuris, M. Heyns. Microelectron. Eng., **80**, 6, (2005). DOI: 10.1109/ESSDER.2004.1356521

[22] J. Liu, L. Gu, N. Cui, S. Bai, S. Liu, Q. Xu, Y. Qin, R. Yang, F. Zhou. Nanoscale Res. Lett., **14**, 1 (2019).

[23] B. Vincent, R. Loo, W. Vandervorst, J. Delmotte, B. Douhard, V.K. Valev, M. Vanbel, T. Verbiest, J. Rip, B. Brijs, T. Conard, C. Claypool, S. Takeuchi, S. Zaima, J. Mitard, B. De Jaeger, J. Dekoster, M. Caymax. Solid-State Electron., **60** (1), 116 (2011). DOI: 10.1016/J.SSE.2011.01.049

[24] T. Nagashima, K. Hokoi, K. Okumura, M. Yamaguchi. IEEE 4th World Conf. Photovoltaic Energy Conf., 656 (2006). DOI: 10.1109/WCPEC.2006.279540

[25] N.E. Posthuma, J. van der Heide, G. Flamand, J. Poortmans. IEEE Transactions Electron Devices, **54** (5), 1210 (2007). DOI: 10.1109/TED.2007.894610

[26] V.P. Kishore, P. Paramahans, S. Sadana, U. Ganguly, S. Lodha. Appl. Phys. Lett., **100**, 142107 (2012). DOI: 10.1063/1.3700965

[27] M.A. Putyato, N.A. Valisheva, M.O. Petrushkov, V.V. Preobrazhenskii, I.B. Chistokhin, B.R. Semyagin, E.A. Emel'yanov, A.V. Vasev, A.F. Skachkov, G.I. Yurko, I.I. Nesterenko. Tech. Phys., **64**, 1010 (2019). DOI: 10.1134/S106378421907020X

[28] Pat. 2787955 S1 Rossijskaya Federatsiya, MPK H01L 31/18, B.N. Samsonenko, N.A. Koroleva. Zayavitel' i patentoobladatel' AO „Saturn" (RF); zayavl. 15.09.2021; opubl. 13.01.2023. (in Russian)

[29] Pat. RU 2703840 S1 Rossijskaya Federatsiya, MPK H01L 31/18, B.N. Samsonenko. Zayavitel' i patentoobladatel' AO „Saturn" (RF); zayavl. 10.01.2019; opubl. 22.10.2019.

[30] Pat. 2589517 S1 Rossijskaya Federatsiya, MPK H01L 21/306, B.N. Samsonenko. Zayavitel' i patentoobladatel' AO „Saturn" (RF) and „Raketnokosmicheskij tsentr „Progress" (AO „RKTs „Prigress") (RF); zayavl. 23.04.2015; opubl. 10.07.2015.
[31] Sh. Kagawa, T. Mikawa, T. Kaneda. Jpn. J. Appl. Phys., **21** (11), 1616 (1982). DOI: 10.1143/JJAP.21.1616
[32] E.A. Emelyanov, A.G. Nastovjak, M.O. Petrushkov, M.Yu. Esin, T.A. Gavrilova, M.A. Putyato, N.L. Schwartz, V.A. Shvets, A.V. Vasev, B.R. Semyagin, V.V. Preobrazhenskii. Tech. Phys. Lett., **46**, 161 (2020). DOI: 10.1134/S1063785020020194
[33] I. Jiménez, F.J. Palomares, J. Avila, M.T. Cuberes, F. Soria, J.L. Sacedón, K. Horn. J. Vac. Sci. Technol. A., **11**, 1028 (1993). DOI: 10.1116/1.578808
[34] V.V. Filippov, A.N. Vlasov, E.N. Bormontov. Kondensirovannye sredy i mezhfaznye granitsy, **12** (3), 282 (2010). (in Russian).

*Translated by I.Mazurov*